

# Constant-Energy Synchronous Scan and Excitation Emission Matrix Shpol'skii Spectroscopy for Characterization of PAHs

J. W. Hofstraat<sup>1,3</sup> and U. P. Wild<sup>2</sup>

Received January 25, 1998; Accepted June 18, 1998

Polynuclear aromatic hydrocarbons (PAHs) are a vast class of organic compounds. Many PAHs show carcinogenic effects, which in general are strongly dependent on their molecular structure. Hence, some, even structurally strongly related, PAHs may show a large difference in carcinogenicity. Low-temperature fluorescence spectroscopy of PAHs embedded in a polycrystalline *n*-alkane matrix (or Shpol'skii matrix) is a powerful technique to identify trace amounts of PAHs in complex samples. The fluorescence spectra show vibrational resolution, so that even very similar isomers can be discerned. Since the Shpol'skii effect is matrix-induced, both the fluorescence emission and excitation spectra display narrow lines, so that a maximum of information can be obtained via the application of fluorescence excitation–emission matrices. To demonstrate the possibilities of “high-resolution excitation–emission matrices (HREEMs),” a marine sediment sample has been investigated, containing, among others, benzo[*a*]pyrene and benzo[*k*]fluoranthene, PAHs with very similar spectral features, but the former being a notorious carcinogenic compound. The two PAHs could be clearly distinguished in the HREEM. Subsequently, a comprehensive set of data was obtained with a multitude of combinations of excitation and emission wavelengths, which allows for the screening of many PAHs, including all priority pollutants, in one analysis step. A simpler and also highly informative screening method, which can be applied over a wide wavelength region, is that of synchronous scanning: the fluorescence signal is obtained by scanning the excitation and emission monochromators simultaneously. When a fixed wavenumber difference is maintained during the scan, the screening can be done based on structural characteristics of the molecules of interest. High-resolution constant-energy fluorescence (CESF) spectroscopy also has been applied to acquire vibrationally resolved spectra for PAHs in the marine sediment sample. When a relatively small energy difference ( $<800\text{ cm}^{-1}$ ) is applied between excitation and emission wavelength, simple CESF spectra are obtained, which allow for rapid and specific screening of PAHs. Larger energy differences lead to more complex spectra, with spectral features showing up due to various combinations of vibronic excitation and vibronic emission of the same molecule.

**KEY WORDS:** Shpol'skii spectroscopy; fluorescence; polynuclear aromatic hydrocarbons; PAHs; marine sediment; excitation–emission matrix; total luminescence spectroscopy; synchronous scan.

## INTRODUCTION

Conventional, room-temperature, absorption, and emission spectra of polycyclic aromatic hydrocarbons

(PAHs) yield broad and structureless bands. Hence, such spectra do not give much information on the identity of the compounds, which may be used for identification and accurate quantification of the PAH compounds. Just for this type of environmental contaminant it is necessary to be able to perform the determinations with a high degree of specificity: strongly related structures—with very similar electronic spectra at room temperature—may show completely different toxicological effects. The use of low-temperature luminescence methods, in particular, for PAHs embedded in polycrystalline *n*-alkane

<sup>1</sup> Akzo Nobel Central Research, Arnhem, The Netherlands.

<sup>2</sup> Swiss Federal Institute of Technology, Physical Chemistry Laboratory, ETH-Zentrum, CH-8092 Zürich, Switzerland.

<sup>3</sup> To whom correspondence should be addressed at Philips Research, Prof. Holstlaan 4, NL-5656 AA Eindhoven, The Netherlands and University of Amsterdam, Institute of Molecular Chemistry, Nieuwe Achtergracht 129, NL-1018 WS Amsterdam, The Netherlands.

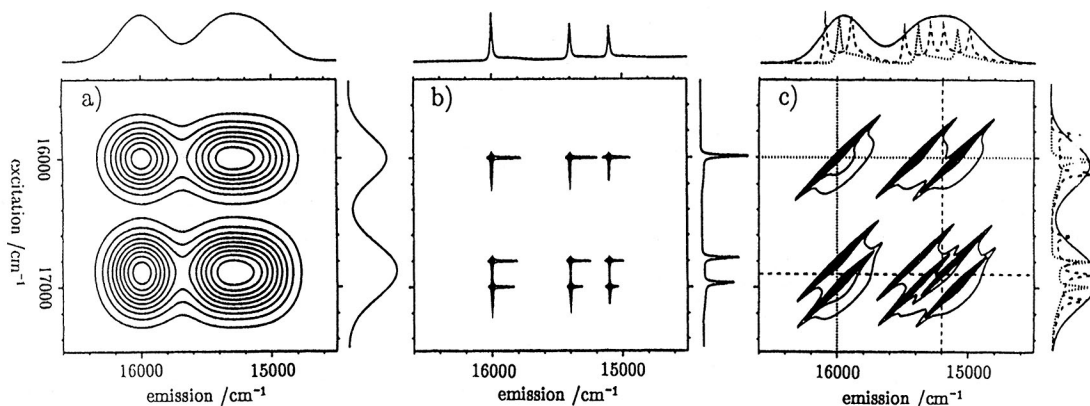


Fig. 1. Schematic diagram of EEM as obtained for a molecule (a) in liquid solution or in an amorphous matrix under nonselective excitation, (b) in a Shpol'skii matrix, and (c) in a cryogenic, amorphous, solution under selective excitation.

matrices which present a highly ordered crystalline environment to the guest molecules on a molecular level, allows for the measurement of highly resolved spectra allowing for specific identification. Via the so-called Shpol'skii method, named after its Russian inventor, Evgenii Shpol'skii, vibrationally resolved spectra are obtained with fingerprint specificity like infrared or Raman spectra, but obtained with the same level of sensitivity as fluorescence spectra [1]. Particularly for the determination of the, generally strongly fluorescent, PAHs, such methods have proven to be very useful [2–4]. In contrast to also applied laser site selection (or fluorescence line narrowing) techniques, where selective optical excitation results in the formation of a well-defined subset of excited molecules [1], the vibrationally resolved fluorescence spectra in Shpol'skii spectroscopy are attributable solely to a homogenization of the local structure of the host material. Therefore both absorption (excitation) and emission spectra show narrow lines. The highly resolved character of the excitation spectrum has been exploited for further selectivity and sensitivity enhancement in “laser-excited Shpol'skii spectroscopy” [5,6].

The ultimate specificity is obtained by making use of an excitation–emission matrix (EEM) approach. The EEM, also referred to as the total luminescence spectrum (TLS) or two-dimensional spectrum (TDS), comprises all information from the excitation and emission spectra of the fluorescent molecules [7–10]. The EEM is obtained by measurement of luminescence intensities for all kinds of combinations of fluorescence emission and excitation frequency in a certain interval:

$$I_{\text{lum}} = I_{\text{lum}}(\nu_{\text{ex}}, \nu_{\text{em}}) \quad (1)$$

Depending on the nature of the solvent, roughly three

types of EEMs can be obtained, as depicted schematically in Fig. 1 in the form of an isointensity plot. The EEM in Fig. 1a is obtained for a fluorescent molecule in a liquid solution or in a completely amorphous matrix under nonselective, broad-band excitation. For a compound obeying Kasha's rule which emits from a completely relaxed state, the EEM can be represented as the simple product of the emission and excitation spectra obtained under conventional conditions:

$$I(\nu_{\text{ex}}, \nu_{\text{em}}) = k \cdot S_{\text{em}}(\nu_{\text{em}}) \cdot S_{\text{ex}}(\nu_{\text{ex}}) \quad (2)$$

where  $S_{\text{em}}(\nu_{\text{em}})$  and  $S_{\text{ex}}(\nu_{\text{ex}})$  represent the one-dimensional (1-D) emission and excitation spectra, respectively. The 1-D spectra are depicted along the sides of the EEM plot. In Fig. 1b the EEM acquired for a molecule in a Shpol'skii matrix is shown [11]. The lines are narrow and exhibit a weak shoulder to the low-energy side in emission and to the high-energy side in excitation, resulting from coupling of the electronic transitions to the matrix vibrations (electron–phonon coupling). Again, the EEM can be represented by the formula given in Eq. (2); the corresponding 1-D spectra are shown at the side of the EEM. The third EEM, shown in Fig. 1c, is obtained when selective excitation is applied of molecules in an amorphous, cryogenic, medium [11]. The excitation wavelength determines the location and the shape of the—narrow-line—emission spectrum. Now no simple relation can be made between the conventional 1-D spectra (which in fact consist of the summed contributions of many narrow line spectra), and Eq. (2) cannot be applied. In Shpol'skii spectra sometimes contributions are noted from molecules in amorphous sites; in such cases a combination of the EEMs depicted in Figs. 1b and c may be expected.

EEMs have been applied for the study of PAHs in liquid solution, e.g., by the group of McGown (in combination with a fluorescence lifetime filter) [12–14]. The application of low-temperature EEMs has been reported by Wild and co-workers, in combination both with Shpol'skii matrices and with selective excitation approaches [9,11,15]. The application of low-temperature EEMs for determination of PAHs in environmental samples has not been reported before.

On the basis of EEMs, on the one hand, very selective determinations of selected PAHs can be achieved, but on the other hand, simplified detection schemes can be devised. Since the complete 2-D fluorescence spectrum of the mixture of PAHs present in a particular sample is observed in the EEM, optimum conditions for synchronous scan fluorescence measurements (i.e., the optimum wavelength or wavenumber difference between excitation and emission monochromators) can be chosen at a glance. Particularly, low-temperature constant-energy synchronous scans (CESSs) are useful for detection of PAHs and PAH derivatives, since one may focus on structural characteristics, based on the selective detection of a characteristic vibration. Some examples are  $\Delta\nu = 1600 \text{ cm}^{-1}$  for aromatic compounds,  $\Delta\nu = 1700 \text{ cm}^{-1}$  for compounds containing a carbonyl group, and  $\Delta\nu = 1200 \text{ cm}^{-1}$  for compounds containing C–F bonds. Constant-energy synchronous fluorimetry has been pioneered by the group of Winefordner [16,17].

## EXPERIMENTAL

### Instrumental

EEMs were recorded with a high-resolution, computer-controlled spectrometer using photon-counting detection. For excitation the output of a 2.5-kW high-pressure xenon lamp was passed first through a water filter and then through a SPEX 0.85-m double monochromator. Detection was performed with a similar monochromator for separation of the fluorescence light followed by a RCA 31034 photomultiplier tube as single-photon detector. The experiment was controlled by a modified DEC PDP11/73A computer that ran the monochromators and acquired the data points at equidistant points (in wavenumbers). The spectra were corrected for the wavelength dependence of the excitation light intensity using a concentrated solution of oxazine-1-perchlorate in ethanol as a quantum counter (in the 350- to 690-nm interval). The emission light of the quantum counter solution was guided through an optical fiber to a Hamamatsu R928 photomultiplier tube, operated in single-

photon counting mode. The measurement of the quantum counter was also controlled by the computer. The resolution of the low-temperature spectra which have been obtained is determined mostly by the instrumental bandwidths of the excitation and emission monochromators, which was 0.2–0.3 nm for most experiments. For Shpol'skii spectroscopy this is a relatively large bandwidth, but it was required due to the low throughput of the high-resolution monochromators. To keep the data acquisition time within limits, experiments were focused on limited spectral regions, e.g., around 400 nm for benzo[*k*]fluoranthene and benzo[*a*]pyrene and around 360 nm for chrysene. Typical high-resolution EEMs of about 30,000 data points were recorded in about 12 h, with a 1-s sampling time per point.

The sample was contained in an Oxford Instruments CF204 helium flow-through cryostat, which can be operated in the 3–300 K temperature range; the experiments reported here were recorded at a temperature varying from 6 to 10 K. Front-face illumination and detection was applied.

### Materials

Experiments were done on the National Research Council of Canada standard reference material HS-6, originating from a polluted harbor in Nova Scotia. The materials were freeze dried, sieved over 125- $\mu\text{m}$  mesh, and homogenized. PAH concentrations were determined by the NRCC Atlantic Research Laboratory in Halifax, Canada; typical concentrations for the priority pollutants chrysene, benzo[*a*]pyrene, and benzo[*k*]fluoranthene are  $2.0 \pm 0.3$ ,  $2.2 \pm 0.4$ , and  $1.43 \pm 0.15 \mu\text{g/g}$  sediment, respectively. About 2 g of dry sediment was extracted in a Soxhlet apparatus with acetone/hexane, 1:3 (during 4 h at 80°C). The crude extracts with PAHs at  $10^{-6}$ – $10^{-7}$  M concentrations were carefully transferred to a solution in the same volume of *n*-octane (from Janssen Chimica) using a mild nitrogen stream. Care was taken not to remove the solvent completely.

## RESULTS AND DISCUSSION

### Excitation–Emission Matrices

To demonstrate the applicability of EEMs for analysis of PAHs in view of the time-consuming data acquisition, it was decided to focus on the analysis of the two priority pollutants, benzo[*a*]pyrene and benzo[*k*]fluoranthene. The former is known as a highly carcinogenic compound, in contrast to the latter [18]. The two

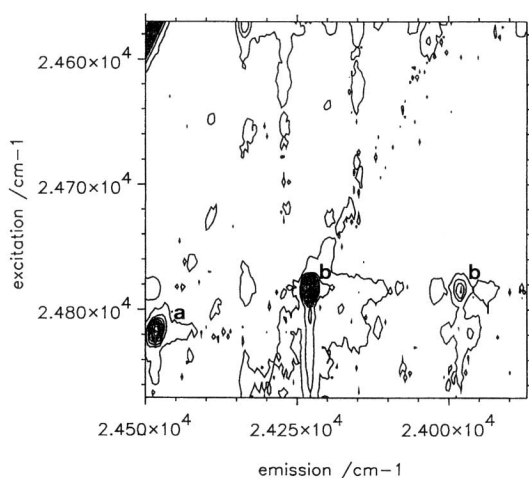


**Fig. 2.** Excitation–emission matrix obtained for the marine sediment extract by scanning the excitation monochromator from 23,670 to 22,870  $\text{cm}^{-1}$  and the emission monochromator from 24,870 to 24,570  $\text{cm}^{-1}$ . Main peaks are indicated: (a) benzo[*a*]pyrene and (b) benzo[*k*]fluoranthene.

PAHs exhibit fluorescence in the same wavelength region, around 400 nm. On the basis of their conventional, broad-band, spectral characteristics, they can hardly be distinguished, but their Shpol'skii spectra provide sufficient resolution to identify and quantify them independently. The  $S_1-S_0$  0–0 transition of benzo[*a*]pyrene in *n*-octane is found at 403.0 nm; that of benzo[*k*]fluoranthene, at 403.5 nm. Major vibronic emission bands are observed at 408.5 nm for benzo[*a*]pyrene and at 412.8 nm for benzo[*k*]fluoranthene.

Figure 2 shows the EEM obtained by scanning the excitation monochromator from 23,670 to 22,870  $\text{cm}^{-1}$ , and the emission monochromator from 24,870 to 24,570  $\text{cm}^{-1}$ . The spectrum indeed shows the features as predicted in Fig. 1. Major Shpol'skii bands are observed at an excitation wavenumber of 24,818  $\text{cm}^{-1}$  and an emission wavenumber of 24,480  $\text{cm}^{-1}$  (peak a, benzo[*a*]pyrene; vibronic band at 338  $\text{cm}^{-1}$ ) and at an excitation wavenumber of 24,782  $\text{cm}^{-1}$  and emission wavenumbers of 24,230 and 23,980  $\text{cm}^{-1}$  (peaks b and c, benzo[*k*]fluoranthene; vibronic bands at 552 and 802  $\text{cm}^{-1}$ , respectively). In addition, some weaker bands are observed, due to other vibronic transitions. The two PAHs are clearly distinguishable due to the highly specific combination of narrow excitation and emission bands. In addition to the typical “spikes” obtained for the molecules embedded in the crystalline, Shpol'skii matrix, some additional features are noted. The weak features extending from the spikes along the excitation and emission axes are due to electron–phonon coupling, coupling between electronic

transitions of the PAH guest molecules with the collective matrix vibrations or phonons. For benzo[*a*]pyrene and benzo[*k*]fluoranthene in *n*-octane, the electron–phonon coupling is weak. In addition, some weak slanting bands are observed, which also comprise the spikes. These bands are due to the selective excitation of the PAH molecules which occupy noncrystalline amorphous sites [19]. The excitation wavelength in that case determines the position of the emission peak, in the so-called fluorescence line-narrowing or fluorescence site selection spectrum [1]. The spectrum is narrow along the emission or along the excitation axis, but a synchronous scan shows the heterogeneously broadened spectrum. The intense feature in the upper left-hand corner is due to scatter from the matrix: the excitation and emission wavenumbers approach each other and the polycrystalline matrix produces significant Rayleigh scatter.

The interpretation given above can be further illustrated when the EEM is cut at the excitation wavenumbers 24,817.3 and 24,783.4  $\text{cm}^{-1}$ , respectively, the 0–0 transitions of benzo[*a*]pyrene and benzo[*k*]fluoranthene, as shown in Fig. 3. The main peaks described above are easily identified. From the spectra the spectral bandwidth can be estimated. For both PAHs it amounts to approximately 20  $\text{cm}^{-1}$  full width at half-maximum (FWHM), which is clearly dominated by the instrumental conditions. The instrumental bandwidth is 12  $\text{cm}^{-1}$ , and the step size 5  $\text{cm}^{-1}$ , for the spectra depicted in Figs. 2 and 3. The relatively large bandwidth and stepsize are required to keep the total spectral acquisition time within reasonable limits. The EEM in Fig. 2 is composed of almost 10,000 points, which has been measured with a dwell time of 1 s. In combination with the time needed to scan the monochromators, the total time needed to obtain the EEM is about 6 h.

### Constant-Energy Synchronous Fluorescence

An alternative approach is to record a constant-energy synchronous fluorescence (CESF) scan of the sample. Synchronous fluorometry is well known as a method for selective measurement of PAHs; in the most-applied approach a constant wavelength difference is used between the excitation and the emission monochromators, which are scanned in tandem [20]. The main advantage of the CESF scan over conventional synchronous fluorescence methods is that the constant wavenumber difference reflects the vibrational structure of the analyte. The wavenumber spectrum reflects the energy levels of the molecules. The CESF can therefore be applied to monitor a particular structural feature of the analytes, by choosing a wavenumber difference which represents a

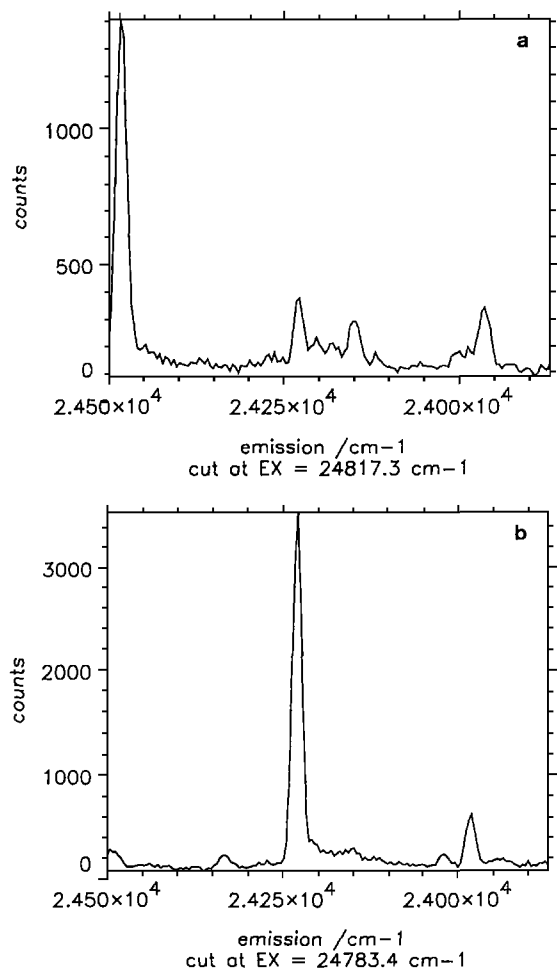


Fig. 3. Cut of the EEM shown in Fig. 2 at excitation wavenumbers  $24,817\text{ cm}^{-1}$  (benzo[*a*]pyrene 0–0 transition) and  $24,783\text{ cm}^{-1}$  (benzo[*k*]fluoranthene 0–0 transition).

vibrational mode. In the EEM it was observed that a characteristic frequency for a ground-state vibrational mode of benzo[*k*]fluoranthene was  $552\text{ cm}^{-1}$ . Therefore a CESF scan was made with a constant energy difference of  $550\text{ cm}^{-1}$  between the excitation and the emission wavenumbers. The excitation wavenumber was scanned from  $28,000\text{ cm}^{-1}$  ( $357\text{ nm}$ ) to  $16,000\text{ cm}^{-1}$  ( $625\text{ nm}$ ). The CESF obtained is shown in Fig. 4. A large number of well-resolved peaks are observed across this wide wavenumber range. Let us focus on the  $25,000\text{--}23,000\text{ cm}^{-1}$  region, where the resonances of benzo[*a*]pyrene and benzo[*k*]fluoranthene are expected. Four major peaks are noted. The first peak (a, excitation at  $25,374\text{ cm}^{-1}$ , emission at  $24,824\text{ cm}^{-1}$ ) corresponds to excitation in an excited-state vibronic band of benzo[*a*]pyrene and subsequent 0–0 emission. The second peak (b, excitation

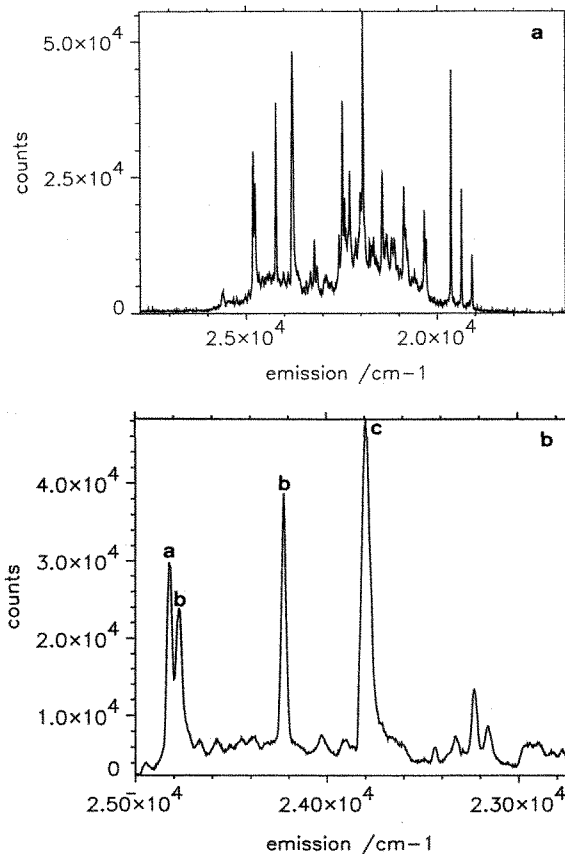


Fig. 4. Constant-energy synchronous fluorescence scan obtained by scanning the excitation monochromator from  $28,000$  to  $16,000\text{ cm}^{-1}$  at a constant-energy difference of  $550\text{ cm}^{-1}$  between excitation and emission monochromator.

at  $25,327\text{ cm}^{-1}$ , emission at  $24,777\text{ cm}^{-1}$ ) corresponds analogously to vibronic excitation and 0–0 emission for benzo[*k*]fluoranthene. The third peak (b, excitation at  $24,778\text{ cm}^{-1}$ , emission at  $24,228\text{ cm}^{-1}$ ) can be attributed to 0–0 excitation followed by vibronic emission of benzo[*k*]fluoranthene; benzo[*a*]pyrene does not have a significant transition corresponding to a  $550\text{ cm}^{-1}$  vibrational mode in the ground state and is, therefore, not observed. The strongest band in the CESF is found for excitation at  $24,344\text{ cm}^{-1}$  and emission at  $23,794\text{ cm}^{-1}$ . This peak, c, is due to benzo[*g,h,i*]fluoranthene; a vibronic excitation and the 0–0 emission of this compound exactly match the observed excitation and emission wavenumbers. The NRCC datasheet of the SRM unfortunately mentions only the EPA priority pollutants, to which benzo[*g,h,i*]fluoranthene does not belong. Figure 4 shows a number of additional bands, which may be identified as well.

The interpretation of a CESF scan with a wavenumber difference of  $550\text{ cm}^{-1}$  is fairly simple, since not many transitions are found in the highly resolved fluorescence spectra which represent such a relatively small difference in energy. The number of allowed vibronic transitions with such a low vibrational energy is low in PAHs. Most bands therefore can be attributed either to vibronic excitation and 0–0 emission or to 0–0 excitation and vibronic emission. When larger energy differences are applied, other combinations of excitation and emission wavenumbers become possible, e.g., vibronic excitation in combination with vibronic emission. Fortunately, in general the oscillator strength of 0–0 transitions is significantly larger than that of vibronic transitions, so that the most intense bands can be easily attributed. The use of EEMs obviously is very helpful for the interpretation of the CESF scans, because the signals can be comprehensively evaluated. Obviously, the advantage of CESF over HREEM is that a significantly shorter acquisition time is needed to obtain the desired information.

## CONCLUSION

HREEMs of fluorescent molecules in low-temperature Shpol'skii matrices can be applied to obtain highly specific vibrationally resolved fingerprints, which are useful to identify trace contaminants in environmental samples. Even molecules with similar spectral characteristics can be distinguished on the basis of such spectra, as has been demonstrated by the example of a harbor sediment sample containing benzo[*a*]pyrene and benzo[*k*]fluoranthene, the former being a notorious carcinogenic compound. A comprehensive set of data is obtained with combinations of excitation and emission wavenumbers, which allows for the screening of many PAHs, including all priority pollutants, in one analysis step. The acquisition of HREEMs is time-consuming, unless special instrumental setups are applied, which are comprised of parallel excitation and detection hardware (e.g., distributed excitation using prisms and parallel detection with an intensified CCD detector). However, such hardware is not easily prepared so that high-resolution data are obtained; at least a resolution of the order of 1-nm is required to get vibrational resolution in fluorescence spectra. New developments like Optical Parametric Oscillators, intense laser sources with a very broad tuning curve of adequate linewidth for high-resolution spectroscopy, enable one to obtain laser-excited HREEMs, which couple the specificity of the high-resolution excitation–emission matrices to the high sensi-

tivity afforded by the high-intensity excitation source. For practical applications in environmental analysis, in particular, when a limited number of pollutants with well-characterized spectral features are to be determined, sufficient specificity can be attained by straightforward 1-D high-resolution spectra, as has been demonstrated by the excitation and emission cuts in the EEM in Fig. 1. In particular, laser-excited Shpol'skii spectroscopy (LESS) [5,6] is a powerful and distinctive, and at the same time sensitive, technique for such applications.

An alternative way to get fingerprint data over a wide wavelength region in a single scan is by synchronous fluorescence spectroscopy. High-resolution CESF can be applied to obtain vibrationally resolved spectra for many PAHs as well, at a significantly shorter acquisition time than HREEMs. When a relatively small energy difference ( $<800\text{ cm}^{-1}$ ) is applied between excitation and emission wavenumber, simple CESF spectra are obtained, which allow for rapid and specific screening of PAHs in environmental samples. Larger energy differences lead to more complex spectra, with spectral features showing up due to various combinations of vibronic excitation and vibronic emission of the same molecule. For the interpretation of such complex spectra it is useful to have HREEM data available, which allow the straightforward identification of peaks derived from one species. Once such identifications have been made, obviously CESF can be applied without further need of HREEM "background information."

## REFERENCES

1. J. W. Hofstraat, C. Gooijer, and N. H. Velthorst (1988) in S. G. Schulman (Ed.), *Molecular Luminescence Spectroscopy: Methods and Applications—Part II*, Wiley, New York, pp. 283–400.
2. J. W. Hofstraat, H. J. M. Jansen, G. Ph. Hoorweg, C. Gooijer, N. H. Velthorst, and W. P. Cofino (1985) *Int. J. Environ. Anal. Chem.* **21**, 299–332.
3. J. W. Hofstraat, W. J. M. van Zeijl, F. Ariese, J. W. G. Mastenbroek, C. Gooijer, and N. H. Velthorst (1991) *Marine Chem.* **33**, 301–320.
4. P. Garrigues, M.-P. Marniesse, S. A. Wise, J. Bellocq, and M. Ewald (1987) *Anal. Chem.* **59**, 1695–1700.
5. Y. Yang, A. P. D'Silva, and V. A. Fassel (1981) *Anal. Chem.* **53**, 894–899.
6. F. Ariese, S. J. Kok, C. Gooijer, N. H. Velthorst, and J. W. Hofstraat (1993) in P. Garrigues and M. Lamotte (Eds.), *Polynuclear Aromatic Hydrocarbons: Synthesis, Properties, Analysis, Occurrence, and Biological Effects*, Gordon and Breach, London, pp. 761–768.
7. G. D. Christian, J. B. Callis, and E. R. Davidson (1981) in E. L. Wehry (Ed.), *Molecular Fluorescence Spectroscopy, Vol. 4*, Plenum Press, New York, pp. 111–165.
8. I. M. Warner, G. Patonay, and M. P. Thomas (1985) *Anal. Chem.* **57**, 463A–483A.
9. A. J. Kallir, G. W. Sutter, S. E. Bucher, E. Meister, M. Lüönd, and U. P. Wild (1987) *Acta Phys. Polonica A71*, 755–764.

10. T. T. Ndou and I. M. Warner (1991) *Chem. Rev.* **91**, 493–507.
11. J. W. Hofstraat, R. Locher, and U. P. Wild (1990) *Appl. Spectrosc.* **44**, 1317–1325.
12. D. W. Millican and L. B. McGown (1988) *Appl. Spectrosc.* **42**, 1084–1089.
13. D. W. Millican and L. B. McGown (1989) *Anal. Chem.* **61**, 580–583.
14. D. W. Millican, K. Nithipathikom, and L. B. McGown (1988) *Spectrochim. Acta* **43B**, 629–637.
15. G. W. Suter, E. C. Meister, and U. P. Wild (1988) *SPIE Proc.* **910**, 81–86.
16. E. L. Inman and J. D. Winefordner (1982) *Anal. Chem.* **54**, 2018–2022.
17. L. A. Files, B. T. Jones, S. Hanamura, and J. D. Winefordner (1986) *Anal. Chem.* **58**, 1440–1443.
18. W. Karcher, R. J. Fordham, J. J. Dubois, P. G. J. M. Glaude, and J. A. M. Ligthart (Eds.) (1983) *Spectral Atlas of Polycyclic Aromatic Compounds, Vol. 1*, Reidel/Kluwer, Dordrecht, The Netherlands.
19. J. W. Hofstraat, I. L. Freriks, M. E. J. de Vreeze, C. Gooijer, and N. H. Velthorst (1989) *J. Phys. Chem.* **93**, 184–190.
20. T. Vo-Dinh (1981) *Anal. Chem.* **50**, 396–401.